

Differential diagnosis of Interstitial Lung Diseases using Deep Learning networks

V. N. Sukanya Doddavarapu , Giri Babu Kande & B. Prabhakara Rao

To cite this article: V. N. Sukanya Doddavarapu , Giri Babu Kande & B. Prabhakara Rao (2020): Differential diagnosis of Interstitial Lung Diseases using Deep Learning networks, The Imaging Science Journal, DOI: [10.1080/13682199.2020.1781394](https://doi.org/10.1080/13682199.2020.1781394)

To link to this article: <https://doi.org/10.1080/13682199.2020.1781394>



Published online: 18 Jun 2020.



Submit your article to this journal [↗](#)



Article views: 12



View related articles [↗](#)



View Crossmark data [↗](#)

Differential diagnosis of Interstitial Lung Diseases using Deep Learning networks

V. N. Sukanya Doddavarapu^a, Giri Babu Kande^b and B. Prabhakara Rao^c

^aECE Department, St. Ann's College of Engineering and Technology, Chirala, India; ^bECE Department, VVIT, Nambur, India; ^cECE Department, JNTUK, Kakinada, India

ABSTRACT

An architecture for automatic lung tissue classification method based on the Deep Learning techniques is designed in this paper. Recent works on Deep Learning techniques achieved impressive results in the field of medical image classification. So, we designed a Convolution Neural Network (CNN) for the classification of five categories of Interstitial Lung Diseases (ILD) patterns in High-Resolution Computed Tomography (HRCT) images. The CNN consists of 3 Convolution layers, Leaky ReLU activation followed by Maximum pooling layer and dense layer. The last Fully Connected (FC) layer has 5 outputs equivalent to the classes considered such as Normal, Ground Glass (GG), Emphysema, Micro Nodules, and Fibrosis. The proposed CNN is trained and evaluated on the publicly available ILD database provided by the University Hospitals of Geneva (HUG). Experimental results are compared with the state-of-art, which shows an outstanding performance of the proposed CNN model giving 94.67% accuracy and 94.65% F_{avg} .

ARTICLE HISTORY

Received 16 March 2019
Accepted 5 June 2020

KEYWORDS

Interstitial Lung Disease (ILD); Convolution Neural Network (CNN); lung tissue classification; High-Resolution Computed Tomography (HRCT); Deep Learning; medical image classification; University Hospitals of Geneva (HUG); accuracy

Introduction

Interstitial Lung Diseases (ILD) provides more than 150 different tissue patterns for lung CT images [1]. ILD causes scarring of the lungs and makes it difficult for breathing. By and large, for the treatment of lung sicknesses deciding the kind of turmoil is conveyed by the strategies, for example, Blood test, aspiratory work tests, and HRCT imaging. Presently a day's HRCT imaging is turning into the standard practice as a result of its high picture quality. Distinctive ILDs show diverse tissue designs on HRCT pictures [2] and translating the genuine ILD is basic. It is a challenge even for the trained radiologists to interpret the particular ILD from HRCT images. Depending on the physical conditions and the medical history of the patient for the same ILD different types of lung tissues are present. When the radiologists are under heavy workload to manually identify the type of tissue pattern which is error-prone is difficult. So, it is advised to have an automatic trained system to identify the tissue pattern for interpreting the type of ILD for initial screening.

In this work, we provide the classification of five classes of lung tissue patterns on High-Resolution Computed Tomography (HRCT) images- Normal, Ground Glass (GG), Emphysema, Micro Nodules and Fibrosis which are primary among the types of ILDs. Figure 1 illustrates these five classes of lung tissue patterns for three datasets.

These lung images patches exhibit similar appearance between different tissue categories and also exhibits great variations between the same categories as shown in Figure 1. These tissue patterns are visually not differentiated and exhibit low inter-class distinction and high intra-class variation. As a result, a robust scheme for automatic image patch classification is necessary for the diagnosis of Interstitial Lung Diseases (ILD). As the first part of the section the previous works have done on the classification of interstitial lung diseases (ILD) are discussed. Next, some basics about CNN and its tuning process are explained. And finally, the proposed CNN architecture is designed.

Related work

Medical image classification is carried out in two steps: the first step as feature descriptor extraction based on texture, colour and shape, and second step labelling the tissue patterns using machine learning algorithms. However, large work is carried out to develop an efficient shape, texture, and colour feature extraction for spatial and frequency-based image analysis. The numerical number of methods for extracting visual features is described by [2]. Intensity properties of tissue patterns are explained by gray level values [4,5]. For additional texture feature extraction, second-order statistic filters such as Gray Level Co-Occurrence Matrix

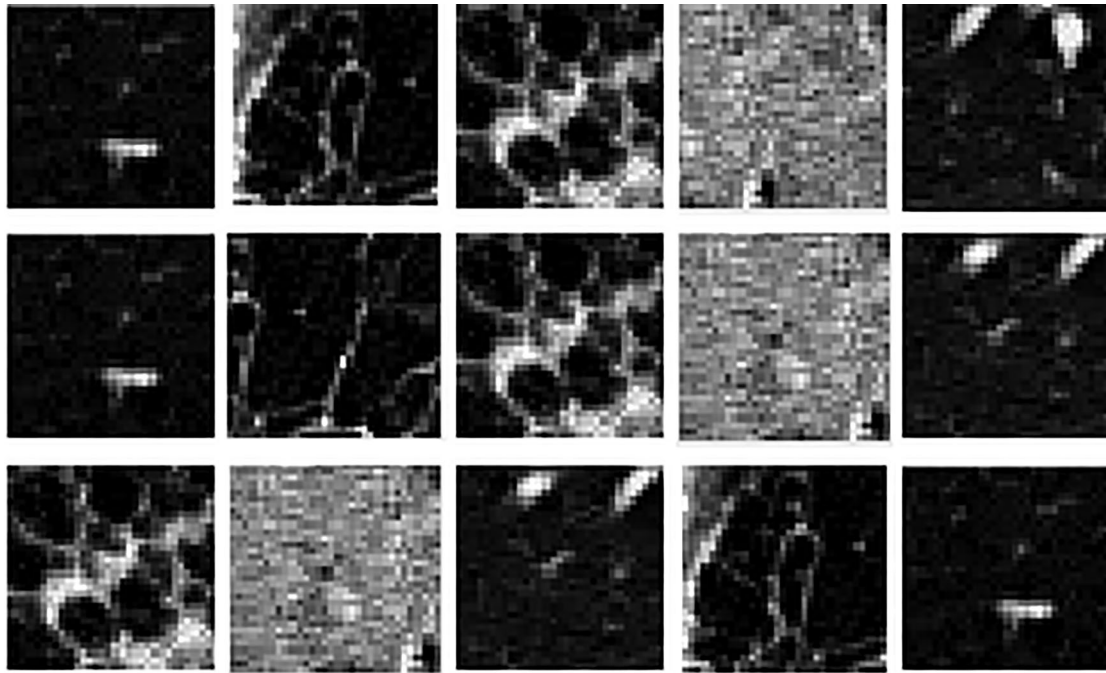


Figure 1. The visual aspect of three sets of images from Talisman Suit [3]. From left to right: Healthy, Emphysema, Ground Glass (GG), Fibrosis, and Micro Nodules.

(GLCM) and (RLE) [6–10] are employed. Edge features are extracted by Gaussian and Wavelet filters [11–15]. To highlight the spatial and shape features [10,13,16], are preferred. Besides, to have multi-variant, multi-resolution texture descriptors to achieve better results for HRCT imaging are described by the Scale Invariant Feature Transform (SIFT) [17,18], Local Binary Patterns (LBP) [12,13], and the Histogram of Oriented Gradients (HOG) [16]. For the given image patch the above-mentioned feature extraction techniques are applied. Figure 2 shows an example of an HRCT lung image with an orange contour indicates (AROI) and the green box indicates the image patch. The annotated region of interest (AROI) has multiple non-overlapping patches among which there is no spatial correlation. That is why we perform patch wise feature extraction.

After obtaining feature descriptors, the next step is to image classification to assign labels to the

descriptors. For labelling, machine learning algorithms are used. In the current work, we focus on supervised approaches. Among them the most frequently used classification methods are Support Vector Machine (SVM) [10], K- Nearest Neighbour (KNN) [9,11,12,15], Bayesian Classifiers [6], Linear Discriminant Analysis (LDA) [13,17], and Artificial Neural Network (ANN) [4]. Among these classifiers SVM gives improved true positive rates and accuracy.

Recent works use unsupervised approaches for extracting learned features from lung tissues to customize the training data. These techniques include sparse representation models [4,17], a bag of features [19] uses k-means and k-SVD to identify the set of textons in the given local patch. RBM [20] used in ANNs produces statistical properties for the given input. Another tool for extracting learned features, multiple kernel learning classifier (m-MKL) [21] uses class-specific dictionaries that minimize the reconstruction error for classification.

The major drawback of machine learning algorithms is, they do pixel classification without considering the local dependency of labels. To account for this, one can employ CNN. Recent works on Deep Learning techniques and especially CNN's achieved impressive results in the field of medical image classification [21]. Unlike the approaches discussed previously CNN's learn features and train the network at the same time by minimizing the loss function. Firstly, shallow architectures are used for lung tissue classification. In [21] (AlexNet) was used for classification. The input is a colour image with size 224×224 , so the authors should resize their image patch into three dimensional by applying

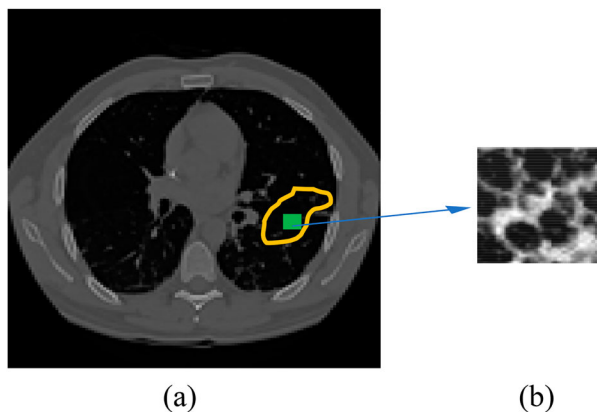


Figure 2. (a) Lung image (512×512) (b) Image patch (32×32).

various Hounsfield unit (HU) windows. Later in [19] the pre-trained CNN [21,22] was used for lung tissue classification. A comparison of shallow and Deep Learning techniques [23] shows less classification error by increasing the number of convolution layers.

Our contribution

As shown in Figure 1, the lung tissue patterns exhibit similarity with the other class and variation within the same class. To solve this problem, in the paper we designed a CNN model that gives superior performance compared to the traditional CNN's used in the previous works. The flow diagram representing the classification for the five categories of lung tissue patterns is as shown in Figure 3. The image patches obtained from the Talisman suit [3] are trained with the CNN Model as in Figure 4. Unlike the pre-trained CNN's [21] and [24], the input layer is designed with the size the same as the image patch. As a result, the classification accuracy is improved.

Proposed CNN Model

Recently, CNN was used in medical image classification because it extracts features and performs classification at the same time giving outstanding results. The Convolution Neural Network (CNN) consists of mainly the Convolution layer, Pooling layer followed by Activation functions, and Fully Connected (FC) layer. The Convolution layer [25,26] produces the features by convolving the input feature maps with the kernels defined in the layer. The feature maps are joined with the past layers with the weights of the kernel. To upgrade the properties of the input layer, the values to the weights are assigned during the training phase. In general Convolution layer have fewer weights compared to the last dense Fully Connected (FC) layer, to make CNN is easy for training. For the easy convergence of the network the weights are assigned by the backpropagation during training. At each output of the unit a non-linear activation is applied. The edge features [27] are enhanced by convolving all features from the initial layers. The following basics are related to CNN is important.

Initialization

Backpropagation gradients will vanish if the network fails to converge during training. To maintain activations and gradients in control levels initialization is done. Here we use Xavier weights with 0.1 bias.

Activations

The purpose of the activation function is to increase the speed of convergence of the CNN network. Initially,

Rectifier linear (ReLU) layer was used. The function is defined mathematically as in Equation (1).

$$f(x) = \max(0, x) \quad (1)$$

In [21], it gave better results more than hyperbolic tangent and classic sigmoid functions, and speed up the training process. The major drawback of this function is, it assigns a constant '0' value, which results in the elimination of all negative values. By the introduction of the Leaky Rectifier Linear layer (Leaky ReLU) the limitations of Equation (1) are overcome. This activation function is defined as in Equation (2), introduces a small slope on the negative part of the function.

$$f(x) = \max(0, x) + \alpha \min(0, x) \quad (2)$$

where α is the leakiness parameter, its default value is 0.01.

Pooling

The purpose of pooling is to reduce the computational load of the successive stages, which is achieved by spatially combining the nearby features [27]. It is classified into two types. (a) Max-pooling: The pixel value is replaced by the maximum value defined in the mask. (b) Average pooling: The pixel value is replaced by the average value defined in the mask.

Regularization

It has done for several reasons. First, it prevents overfitting by applying L1 and L2 regularization. Because of this, we can bound the absolute values of kernel weights. Another regularization method introduced is Dropout [27]. In this method, we can stochastically add noise to hidden layers by multiplying probability value P (e.g. 0 or 0.5) to each unit during the training process. This helps the network to learn the features of their own.

Data augmentation

If the input to the CNN is of different sizes with the input layer, we have to resize the training set by using the process called Data Augmentation. This can be done in two ways either by Translation or Rotation. In [21], image translation is used. This results in less classification accuracy because in the segmentation process rotation should be used. So, we generated the new dataset for classification by rotating the lung tissue patches in angles as the multiples of 90° .

Loss function

The first part of training the CNN is to define the loss function. Equation (3) gives the Categorical Cross-entropy that should be minimized during the training

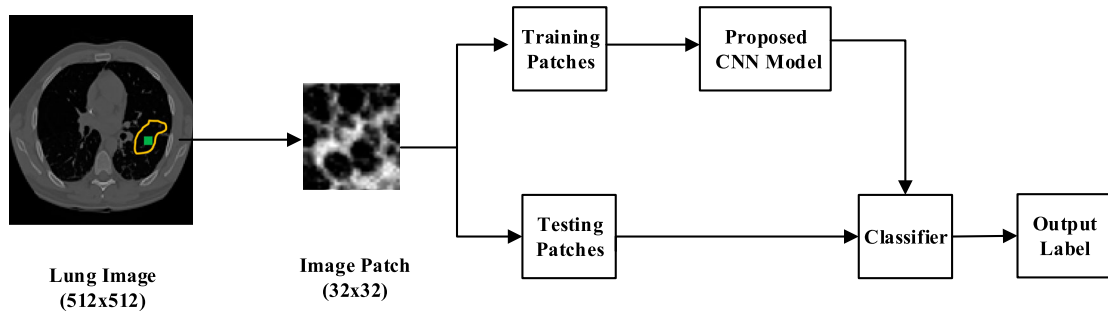


Figure 3. Flow diagram of the proposed classification model.

process.

$$H = - \sum_{j \in \text{voxels}} \sum_{k \in \text{classes}} C_{j,k} \log(\hat{C}_{j,k}) \quad (3)$$

where $\hat{C}_{j,k}$ represents the probabilistic predictions

Architecture

The lung tissue patterns exhibit large variability in intra-class structures and small variability in inter-class structures, which makes the classification a challenging problem. To overcome such complexity, we designed a robust classification CNN Model as shown in Figure 4. The input to the proposed CNN is a 2-D image patch of size 32×32. The first convolution layer is designed to have 5×5 kernels with 16 filters.

The network consists of altogether 3 Convolution layers with the number of filters increased to 32 and 64 respectively. The output of the Convolution layer is followed by the Maximum pooling with kernels of size 2×2 that reduces the size of an image patch by half. Activation functions are used to speed up the process of convergence. Here, instead of the ReLu layer, Leaky ReLu activation was used. Since, Leaky ReLu layer assigns a non-zero value to a negative slope unlike the ReLu layer. The default value for leaky parameter α as 0.01 is changed to 0.3, to increase

the speed of convergence. The proposed CNN is to classify five categories of lung patches. So, the last fully connected layer is designed to classify for 5 outputs.

Training

The training of CNN is done in two steps. As the initial step, we define a loss function and as the second, we interpret an optimization algorithm that minimizes the loss function. In the present work, Adam optimizer [28] is used to minimize the cross-entropy. The cross-entropy is a measure of mismatch among predicted labels with the ground truths.

Implementation

The proposed method is executed on the standard Talisman suit [3] provided by university hospitals of Geneva (HUG). The HUG gives 2-D and 3-D annotated lung tissue patterns to examine multiple cases of interstitial lung diseases (ILD). Different tissue patterns are drawn by 15–20 years of experienced radiologists for 108 image slices of 512×512 pixels/slice. The 2-D AROIs for the image slices are examined to indicate nearly 17 different lung tissue patterns.

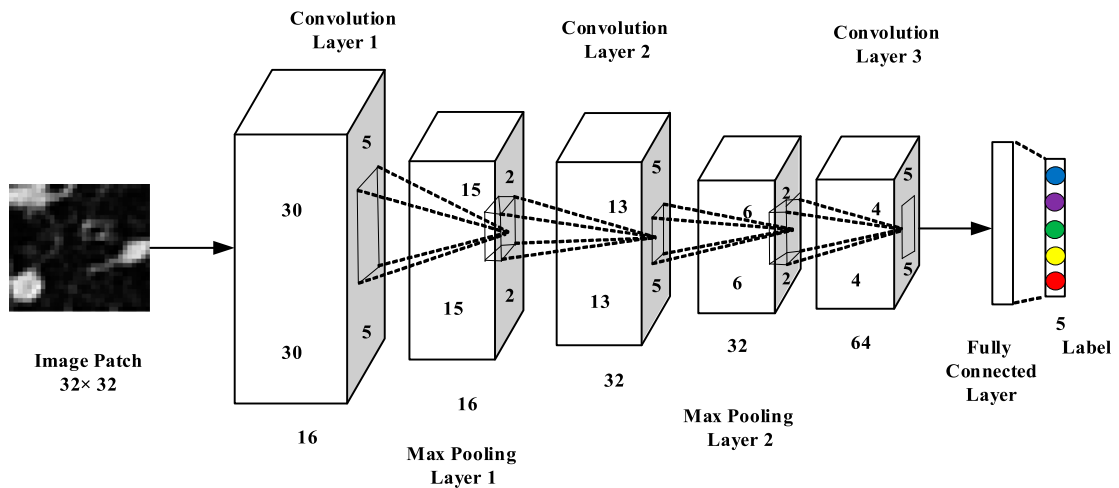


Figure 4. The Topology of the Proposed CNN Model.

Dataset

In the dataset [3], 113 sets of image slices and AROIs of 1458 are given for classification. In our study, we classified five classes of lung tissue patterns such as Normal, Ground Glass (GG), Emphysema, Micro Nodules, and Fibrosis out of 17 tissue patterns. The database is given in Table 1.

For each AROI non-overlapping image patches of 32×32 pixels are drawn because the image patches in the given AROI are not correlated spatially. So, for better classification each image patch is examined in the given AROI. In the Talisman suit the image patches are given as filename_patchnumber_patient number. The filename includes labels. In this work, our proposed two-dimensional methodology is affected by the following criteria: (1) Large spacing between inter slices nearly 10 mm, (2) The provided 2-D AROIs acts as ground truth, and (3) The work is executed on 2-D image slices with the help of the proposed CNN model, as explained in Figure 4. Image patches having centroids outside of annotated AROIs are removed for evaluation. Table 1 gives a total of 23731 image patches for all lung tissue classes.

Evaluation metrics

We compare the classification performance of the proposed CNN model with the hand-crafted techniques as well as the standard CNN's for the given dataset, with measures such as Recall, Precision, F-score, and Accuracy which are defined [29,30] as follows.

$$\text{Recall} = \frac{TP}{TP + FN} \quad (4)$$

$$\text{Precision} = \frac{TP}{TP + FP} \quad (5)$$

$$F - \text{score} = \frac{2TP}{2TP + FP + FN} \quad (6)$$

$$\text{Accuracy} = \frac{TP + TN}{TP + TN + FP + FN} \quad (7)$$

Where TP – Number of True Positives for the classification of lung tissue patterns. Similarly, FP- False Positives, TN- True Negatives, and FN- False Negatives. As explained, for classification 70% of image patches are used for training and 30% for testing. So, each lung tissue pattern is classified on this dataset. The 3-D

AROs are excluded for the present image patch classification.

Therefore, the TP, FP, TN, and FN values could be calculated by integrating all the lung tissue patches in the database.

Set up

The training of CNN has done in two steps. At the initial step, we defined a loss function and as the second, we interpreted an optimization algorithm that minimizes the loss function.

In the present work, Adam optimizer [28] is used to minimize cross-entropy. The cross-entropy is a measure of mismatch among predicted labels with the ground truths. Adam optimizer [28] is a first-order gradient method that minimizes the cross-entropy by tuning three parameters such as exponential decay rates for squared gradient and gradient, learning rate. Table 2 shows the hyperparameters used during the training of CNN.

These parameters are updated by using lower-order moments to optimize the stochastic objective function. After many observations the default values for the three parameters are set to 0.9 and 0.99, and the rest is 0.001. The convolution layer is initialized with a bias of 0.1 and Xavier weights [31]. The minimum batch size is set to 64 to update the weights. In the fully connected layer dropout is set to 50% to reduce overfitting. The training ends depending upon the number of epochs. Here it is set to 500. The performance of the network is evaluated in terms of Accuracy, Precision, Recall, and average F-score.

Results and discussions

Comparison with the state-of-the-art

A comparison of the proposed CNN with the previous works using machine learning algorithms is provided

Table 2. Hyperparameters for training CNN.

Stage	Hyperparameter	Value
Initialization	Bias	0.1
	Weights	Xavier
Leaky ReLU	A	0.3
	P	0.5
Drop out	learning rate	0.001
	Max Epochs	50
	Momentum	0.9
	Minimum Batch size	64

Table 1. Overview of the database.

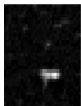




Class	Normal (C _N)	Emphysema (C _E)	Ground Glass (C _G)	Fibrosis (C _F)	Micro Nodules (C _M)
Visual aspect					
Images	15	9	35	35	18
AROs	157	108	416	479	298
Patches	6934	1474	2974	4456	7893

Table 3. Comparison of the proposed CNN with the state-of-the-art.

Method	Features	Classifier	F_{avg}	Accuracy
Gangeh [32]	Intensity	SVM	0.7127	0.7152
Sorensen [12]	LBP + Histogram	-RBF	0.7322	0.7333
Anthimopoulos [18]	Local DCT + Histogram	KNN	0.7786	0.7809
Proposed	CNN Model	RF	0.9465	0.9467

Table 4. Comparison of proposed CNN with other CNN's.

Method	F_{avg}	Accuracy
Li [15]	0.6657	0.6705
LeNet [26]	0.6783	0.6790
AlexNet [21]	0.7031	0.7104
Pre-trained AlexNet [21]	0.7582	0.7609
VGG-Net [24]	0.7804	0.7800
Proposed CNN Model	0.9465	0.9467

in Table 3. The authors extracted the local features as described [12,18,32], where labels are predicted with standard classifiers. In the present work by proper tuning of the hyperparameters as in Table 2, the results bias the performance of the proposed CNN model nearly by 18%.

Comparison with the other CNN's

Table 4 provides a comparison of the proposed CNN with other standard CNNs. Li [15] is the first CNN with 3 Convolution layers and 3 dense layers. It is a shallow architecture that prevents the network from

learning non-linear features results in low accuracy. LeNet [26] has 2 Convolution layers with 6 kernels followed by a Pooling layer with 16 kernels of size 5×5 and 3 dense layers. Next, we evaluated the performance on Alexnet [21] and VGG-Net [24] with 5 and 13 Convolution layers respectively. The input is a colour image with size 224×224 , so the image patch 32×32 is resized into three-dimensional by applying various Hounsfield unit (HU) windows. This results in decreased performance of the pre-trained networks, whereas in the proposed CNN model the input layer is designed with the same size as the input image patch. This results in the biased performance of the network.

Analysis of the system performance

In this graph, we provided additional information about the performance of the proposed method. Figure 5 shows the loss and accuracy curves during the training of the proposed CNN. The red descending curves correspond to the loss function values for the training and validation sets during training. The blue ascending curves correspond to the accuracy values for the training and validation sets during training. The two curves start to diverge from one another to nearly around 100 epochs. However, validation loss continues to descend approximately up to 500 epochs.

Here, we analyze the patch wise lung tissue classification results using our proposed method. Table 5 shows the confusion matrix calculated for the five classes. It measures an average true positive rate of

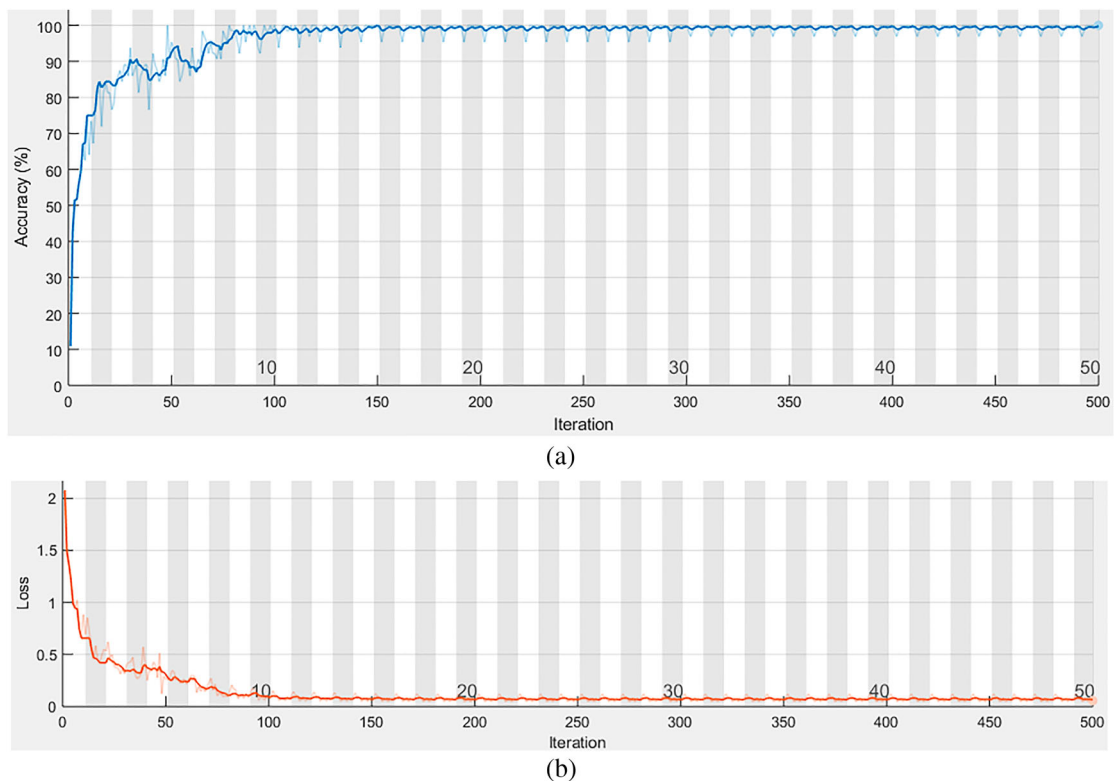
**Figure 5.** (a) Accuracy and (b) Loss curves during the training of the network.

Table 5. Confusion matrix for image patches classification.

Actual classes	Prediction in (%)				
	C_E	C_F	C_G	C_N	C_M
C_E	88.33	0	1.67	3.33	6.67
C_F	1.67	96.67	1.67	0	0
C_G	0	0	95	3.33	1.67
C_N	0	0	0	100	0
C_M	3.33	0	1.67	1.67	93.3

94.67%. The two difficulties which we raised when we are doing classification are low inter-class divergence and high intra-class divergence is reduced by using the proposed CNN model.

Consider the first case similar features exists between C_E and C_N , C_F and C_G , C_M , and C_N . For a small increase of nodule in C_M makes it to identify as the class C_N . C_G patches are highly dense falsely identified as C_F . so, misclassification is expected to occur. Coming to the second case, C_M and C_N have background intensities as high, and become difficult to distinguish. From the confusion matrix for the class Emphysema, 7% wrongly classified as Micro Nodules, since similar features exist between the classes. Figure 6 illustrates the misclassification results among the five lung tissue categories. Similarly, 1.67% of the class Fibrosis is misclassified as Emphysema.

The results of patch wise lung tissue classification in terms of performance measures: Recall, Precision, and F-score are given in Table 6. The average performance

Table 6. Results of image patch classification.

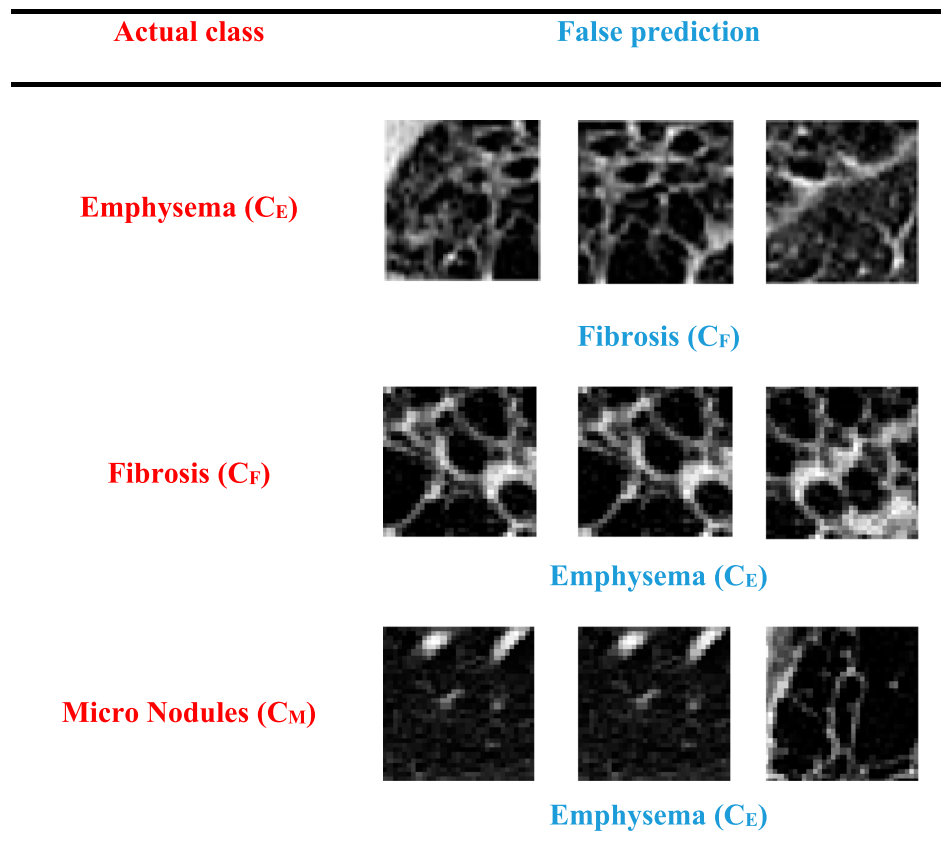
	C_E	C_F	C_G	C_N	C_M	Avg
Precision	94.64	100	95	92.3	91.8	94.75
Recall	88.3	96.67	95	100	93.3	94.67
F-score	91.38	98.3	95	96	92.56	94.65

is nearly 94.67% which shows better performance of our proposed CNN model with the previous methodologies [14,33,34]. The high recall of C_N is because of non- C_N classes are less likely to be mismatched. The low recall of C_E is because of the fewer number of image patches present in the dataset compared to the majority classes.

Our proposed work is implemented with Matlab R2017b, running on a standard personal computer with an I3 processor. For a given image patch the feature vector computation takes 0.06 s and labelling of the image patch for the given five classes takes 0.02s.

Conclusion

We designed a Deep CNN for the classification of lung tissue for the five classes namely Normal, Ground Glass, Emphysema, Micro Nodules, and Fibrosis in the present paper. Our CNN consists of 3 Convolution layers with 5×5 kernels & Leaky ReLU Activation functions followed by a Maximum pooling layer with 2×2 kernels and dense layer. The last Fully Connected (FC) layer

**Figure 6.** The visual aspect of misclassification among the lung tissues Emphysema (C_E), Fibrosis (C_F), and Micro Nodules (C_M).

had five outputs equal to the classes, which were primarily considered. The proposed CNN is trained and evaluated on the publicly available ILD database, which was provided by university hospitals of Geneva (HUG). Results are evaluated with the data set containing 23731 image patches which show outstanding performance.

The results are compared with the popular hand-craft techniques as well as traditional pre-trained CNN networks. The classification accuracy is 94.67%, this is mainly because, in the pre-trained networks [21,24,26], we have to resize the input image patch. In the proposed CNN model, the input layer is of the same size as the image patch. The major drawback of the Deep Learning technique is, the output fluctuates for the same input because of the random variation of weights assigned during the training process. More over classification recall is high for all the classes except Emphysema, this is because of the imbalanced dataset that contains fewer samples for this class. Further, we would like to extend the classification to a greater number of categories and techniques to convert the imbalanced dataset distribution to a balanced dataset.

Disclosure statement

No potential conflict of interest was reported by the author(s).

Notes on contributors

Mrs V. N. Sukanya Doddavarapu is a Ph.D. student of Jawaharlal Nehru Technological University, Kakinada, and working as Assistant Professor of Electronics and Communication Department in St. Ann's College of Engineering and Technology, Chirala. She received her Master's degree in VLSI & ES in the year 2012 from Jawaharlal Nehru Technological University, Kakinada, and Bachelor's degree in Electronics and Communication Engineering in the year 2008 from Acharya Nagarjuna University, A.P., India. Her research interests focus on medical image processing, with specific emphasis on the classification of various lung tissue patterns from CT scan images.

Dr Giri Babu Kande is a Professor and Principal i/c of Electronics and Communication Department in Vasireddy Venkatadri Institute of Engineering and Technology, Guntur. He has teaching experience of about 21 years. His research interests include digital image processing, Machine Learning, and Computer Vision. He received his Ph.D. degree in Digital Image Processing from Jawaharlal Nehru Technological University, Hyderabad in the year 2010. About 2 scholars were awarded Ph.D. under his tutelage. He is a member of various professional chapters and published many research papers in various SCI journals, national and international conferences.

Dr B. Prabhakara Rao was born in the year 1955 at Buchiredypalem, Nellore Dist., A.P., India. He obtained B.Tech. & M.Tech. from S.V. University, Tirupathi with Specializations in Electronics and Communications Engineering (ECE), Electronic Instrumentation, and Communications Systems in the years 1979 and 1981 respectively. Dr Rao received Doctorate

from Indian Institute of Science, Bangalore in the area of Sonar Signal processing in the year 1995. Dr Rao joined as Assistant Professor in the JNT University in the Year 1982 and became Professor in ECE Dept. in the year 2003. He worked as Director (Institute of Science & Technology), Rector, and Vice-Chancellor i/c at JNT University, Kakinada. His current areas of research interest are Optical, Wireless, Microwave and Digital Communications & Image processing. About 35 scholars were awarded Ph.D. under his tutelage. Rao published many research papers in various SCI journals and National and International conferences and is a fellow of many Professional Organizations. Presently he is Vice president of IETE, New Delhi.

ORCID

V. N. Sukanya Doddavarapu  <http://orcid.org/0000-0003-0408-3870>

References

- [1] Webb WR, Muller NL, Naidich DP. High-resolution CT of the lung. Philadelphia (PA): Lippincott Williams Wilkins; 2008.
- [2] Sluimer L, Schilham A, Prokop M, et al. Computer analysis of computed tomography scans of the lung: a survey. *IEEE Trans Med Imaging*. 2006;25(4):385–405.
- [3] Depeursinge A, Vargas A, Platon A, et al. Building a reference multimedia database for interstitial lung diseases. *Comput Med Imaging Graph*. 2012;36(3):227–238.
- [4] Uchiyama Y, Katsuragawa S, Abe H, et al. Quantitative computerized analysis of diffuse lung disease in high-resolution computed tomography. *Med Phys*. 2003;30(9):2440–2454.
- [5] Mendoza CS, Washko GR, Ross JC, et al. Emphysema quantification in a multi-scanner HRCT cohort using local intensity distributions. *Universidad de Sevilla, Spain Brigham and Women's Hospital, Harvard Medical School, USA Pontificia Universidad Católica de Chile, Chile National Jewish Medical and Research Center, USA*; 2012. p. 474–477.
- [6] Xu Y, Sonka M, McLennan G, et al. MDCTbased 3-D texture classification of emphysema and early smoking related lung pathologies. *IEEE Trans Med Imag*. 2006;25(4):464–475.
- [7] Yao J, Dwyer A, Summers RM, et al. Computer-aided diagnosis of pulmonary infections using texture analysis and support vector machine classification. *Acad Radiol*. 2011;18(3):306–314.
- [8] Park SC, Tan J, Wang X, et al. Computer-aided detection of early interstitial lung diseases using low-dose CT images. *Phys Med Biol*. 2011;56:1139–1153.
- [9] Korfiatis PD, Karahaliou AN, Kazantzi AD, et al. Texture-based identification and characterization of interstitial pneumonia patterns in lung multidetector CT. *IEEE Trans Inf Technol Biomed*. 2010;14(3):675–680.
- [10] Bagci U, Yao J, Wu A, et al. Automatic detection and quantification of tree-in-bud (TIB) opacities from CT scans. *IEEE Trans Biomed Eng*. 2012;59(6):1620–1632.
- [11] Sluimer IC, Prokop M, Hartmann I, et al. Automated classification of hyperlucency, fibrosis, ground glass, solid, and focal lesions in high-resolution CT of the lung. *Med Phys*. 2006;33(7):2610–2620.
- [12] Sorensen L, Shaker SB, de Bruijne M. Quantitative analysis of pulmonary emphysema using local binary patterns. *IEEE Trans Med Imag*. 2010;29(2):559–569.

- [13] Jacobs C, Sanchez CI, Saur SC, et al. Computer-aided detection of ground glass nodules in thoracic CT images using shape, intensity and context features. In: Fichtinger G, Martel A, Peters T, editors. *Medical Image Computing and Computer-Assisted Intervention – MICCAI 2011 Lecture Notes in Computer Science*. Vol. 6893. Berlin: Springer; 2011. p. 207–214.
- [14] Depeursinge A, de Ville DV, Platon A, et al. Near-affine-invariant texture learning for lung tissue analysis using isotropic wavelet frames. *IEEE Trans Inf Technol Biomed*. 2012;16(4):665–675.
- [15] Li Q, Cai W, Wang X, et al. Medical image classification with the convolutional neural network. 13th International Conference on Control Automation Robotics & Vision (ICARCV). Vol. 2014. 2014 December. p. 844–848.
- [16] Sluimer C, van Waes PF, a Viergever M, et al. Computer-aided diagnosis in high resolution CT of the lungs. *Med Phys*. 2003;30(12):3081–3090.
- [17] Song Y, Cai W, Zhou Y, et al. Feature-based image patch approximation for lung tissue classification. *IEEE Trans Med Imaging*. 2013;32(4):797–808.
- [18] Anthimopoulos M, Christodoulidis S, Christe A, et al. Classification of interstitial lung disease patterns using local DCT features and random forest. 36th Annu. Int. Conf. IEEE Eng. Med. Biol. Soc., 2014. p. 6040–6043.
- [19] Gao M, Bagci U, Lu L, et al. Holistic classification of CT attenuation patterns for interstitial lung diseases via deep convolutional neural networks. 1st Workshop on Deep Learning in Medical Image Analysis, 2015.
- [20] Vo KT, Sowmya A. Multiple kernel learning for classification of diffuse lung disease using HRCT lung images. *Conf Proc IEEE Eng Med Biol Soc*. 2010;2010:3085–3088.
- [21] Krizhevsky A, Sutskever I, Hinton G. Imagenet classification with deep convolutional neural networks. *Adv Neural Inf Process Syst*. 2012:1097–1105.
- [22] Negahdar M, Beymer D. Lung tissue characterization for emphysema differential diagnosis using deep convolutional neural networks. *Proc SPIE* 2019;10950:109503R.
- [23] Kim GB, et al. Comparison of shallow and deep learning methods on classifying the regional patterns of diffuse lung disease. *J Digit Imaging*. 2018;31(4):415–424.
- [24] Simonyan K, Zisserman A. Very deep convolutional networks for large-scale image recognition. *International Conference on Learning Representations*, 2015.
- [25] Jia Y, Shelhamer E, Donahue J, et al. Caffe: Convolutional Architecture for Fast Feature Embedding, 2014.
- [26] LeCun Y, Bottou L, Bengio Y, et al. Gradient-based learning applied to document recognition. *Proc IEEE*. 1998;86(11):2278–2324.
- [27] Li Q, Cai W, Feng DD. Lung image patch classification with automatic feature learning. *Proc. Annu. Int. Conf. IEEE Eng. Med. Biol. Soc. EMBS*, 2013. p. 6079–6082.
- [28] Kingma DP, Ba JL. Adam: a method for stochastic optimization. *Int. Conf. Learn. Represent*, 2015, p. 1–13.
- [29] Olson DL, Delen D. *Advanced data mining techniques*. 1st ed. Berlin: Springer-Verlag; 2008.
- [30] David MW. Evaluation: from precision, recall and F-measure to ROC, informedness, markedness & correlation. *J Mach Learn Technol*. 2011;2(1):37–63.
- [31] He K, Zhang X, Ren S, et al. Delving deep into rectifiers: surpassing human-level performance on imagenet classification.
- [32] Gangeh MJ, Sørensen L, Shaker SB, et al. A texton-based approach for the classification of lung parenchyma in CT images. In: Jiang T, Navab N, Pluim JPW, et al., editors. *Medical Image Computing and Computer-Assisted Intervention – MICCAI 2010 Lecture Notes in Computer Science*. Vol. 6363. Berlin: Springer; 2010. p. 595–602.
- [33] Anthimopoulos M, Christodoulidis S, Ebner L, et al. Lung pattern classification for interstitial lung diseases using a deep convolutional neural network. *IEEE Trans Med Imaging*. 2016;35(5):1207–1216.
- [34] Bondfale N, Bhagwat DS. Convolutional neural network for categorization of lung tissue patterns in interstitial lung diseases. *Proc. Int. Conf. Inven. Commun. Comput. Technol. ICICCT* 2018, no. Iccict, 2018. p. 1150–1154.